Materials Physics and Mechanics. 2022;49(1): 136-144
Conference materials
http://dx.doi.org/10.18149/MPM.4912022_9

Modeling of PKA energy spectra and the concentration of vacancy clusters in materials irradiated with light ions

N.A. Voronova[1], A.A. Kupchishin[1], A.I. Kupchishin[1,2]✉, T.A. Shmygaleva[2]

[1]Abai Kazakh National Pedagogical University, Dostyk, 13, Almaty, Kazakhstan

[2]Al-Farabi Kazakh National University, 71 Al-Farabi Ave., Almaty, Kazakhstan

✉ ankupchishin@mail.ru

Abstract. The work was carried out within the framework of the cascade-probabilistic method, the essence of which is to obtain and further apply cascade-probabilistic functions. The obtained models make it possible to trace the entire process in development and in the future can be used in industry to obtain materials with predetermined characteristics. The results of the obtained studies can also be used by specialists in the field of solid-state radiation physics, in cosmophysics. The cascade-probability functions, the energy spectra of primary knocked-on atoms (PKA), and the concentration of vacancy clusters in molybdenum irradiated with alpha particles were simulated. Some of their properties and patterns were established. Methods of mathematical analysis, probability theory, and numerical methods were used in the research process.

Keywords: cascade-probability function, energy spectrum, modeling, primary knocked-on atom

Acknowledgments *This research has been funded by the Science Committee of the Ministry of Education and Science of the Republic of Kazakhstan (Grant No. AP08855701).*

Citation: Voronova NA, Kupchishin AA, Kupchishin AI, Shmygaleva TA. Modeling of PKA energy spectra and the concentration of vacancy clusters in materials irradiated with light ions. *Materials Physics and Mechanics*. 2022;49(1): 136-144. DOI: 10.18149/MPM.4912022_9.

1. Introduction

As is known, the main cause of changes in the structure and physicochemical properties of materials during radiation exposure is the formation of defects [1-4]. In contrast to light particles (electrons, photons, etc.), the interaction of ions with matter creates not only isolated Frenkel pairs, as is considered in many papers, but mostly the clusters of vacancies and interstitial atoms [5].

The process of interaction of ions with matter and their passage through matter is a rather difficult task when creating both physical and mathematical models [5-8]. First of all, this is due to a catastrophic increase in the cross-section for their interaction with electrons and atoms of the medium. At the same time, the depth of penetration of particles into materials with an increase in the mass of incident particles decreases sharply. In calculating the cascade-probability functions in this case it is necessary to apply special methods and techniques. A set of types of incident particles and targets is a huge number of variants. In this

© N.A. Voronova, A.A. Kupchishin, A.I. Kupchishin, T.A. Shmygaleva, 2022.
Publisher: Peter the Great St. Petersburg Polytechnic University
This is an open access article under the CC BY-NC 4.0 license (https://creativecommons.org/li-censes/by-nc/4.0/)

case, we can consider different situations where the mass number of incident ions A_1 is less than the mass number of the target A_2, i.e. $A_1 < A_2$, the case when A_1 becomes commensurate with A_2, and finally, very unique processes, with $A_1 > A_2$. As a preliminary analysis shows, all these cases must be taken into account – each of them has its own patterns [9-12].

In addition, using a certain sort of incident particles in a particular material, it is possible to form a predetermined structure and chemical compounds that are rather stable in a wide temperature range [12-16]. Naturally, in this case, the physicochemical properties of such substances will differ from those of the initial materials.

Thus, when considering the passage of ions (including light ions: protons, and alpha particles) through the matter, it is necessary to solve a large variety of physical and mathematical problems [12,17-20]. Most of our work in this direction will be carried out in the framework of the cascade-probability method [12].

2. Calculation method

In this paper, we simulated cascade-probability functions (CPFs), the energy spectra of primary knocked-on atoms (PKA), and the concentration of vacancy clusters in substances irradiated with light ions (protons and alpha particles) taking into account the energy loss. It is assumed that a primary particle formed at a depth of h' interacts with the substance as follows (Fig. 1):

1. A charged particle loses energy for ionization and excitation (the main type of energy loss). These losses are considered continuous during the implantation of the particle into the material.

2. The primary particle forms PKA, at those several interactions creating PKA occur simultaneously with hundreds of interactions with the electrons of the medium (ionization losses).

3. PKA does not form Frenkel pairs (vacancy and interstitial atom) but produces vacancy clusters.

4. For protons, alpha particles, and ions, the nonrelativistic case is considered, the interaction cross-section is selected as the Rutherford cross-section, ionization losses for protons and alpha particles are calculated using the Bethe-Bloch formula, for ions are taken from the tables of parameters of the spatial distribution of ion-implanted impurities (Kumakhov-Komarov).

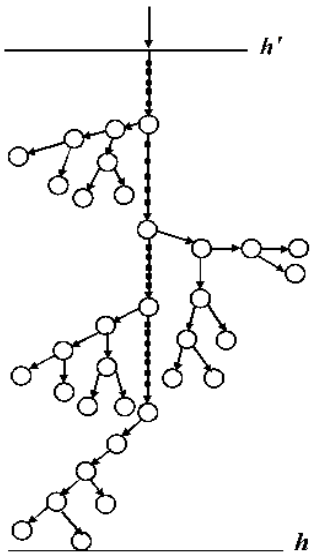

Fig. 1. Physical model of the interaction of ions with target

For protons and alpha particles forming primary knocked-on atoms, the dependence of the cross-section on energy, which, in its turn, depends on the penetration depth, is represented as follows:

$$\sigma(h)=\sigma_0\left(1+\frac{1}{a\left(E_0-kh\right)}\right), \tag{1}$$

where a and E_0 are the approximation parameters obtained by comparing (1) with the calculations of true sections, for example, by electrodynamics methods, by conventional methods, etc.

We have calculated the cascade-probability function (CPF) for ions taking into account the energy loss depending on the interaction parameters. The cascade-probability function, in this case, has the following form (for protons and alpha particles it is the same):

$$\psi_n\left(h',h,E_0\right)=\frac{1}{n!\lambda_0^n}\left(\frac{E_0-kh'}{E_0-kh}\right)^{-l}\exp\left(-\frac{h-h'}{\lambda_0}\right)\left(h-h'+\frac{\ln\left(\frac{E_0-kh'}{E_0-kh}\right)}{ak}\right)^n, \tag{2}$$

where n is the number of interactions, $\lambda_0=1/\sigma_0$, $l=1/\left(\lambda_0 ak\right)$; h', h are the depths of generation and registration, respectively.

PKA spectrum for ions is determined by the following expression:

$$W\left(E_0,E_2,h\right)=\sum_{n=0}^{n_1}\int_{h-k\lambda_2}^{h}\psi_n\left(h'\right)\exp\left(-\frac{h-h'}{\lambda_2}\right)\frac{w\left(E_1,E_2,h'\right)dh'}{\lambda_1\left(h'\right)\lambda_2}. \tag{3}$$

The concentration of vacancy clusters that formed during irradiation of solid with ions is calculated by the formula: max

$$C_k(E_0,h)=\int_{E_c}^{E_{2\max}}W(E_0,E_2,h)dE_2, \tag{4}$$

where E_C is the minimum energy for cluster formation.

3. Results and discussions

As the calculations show, approximation (1) describes the modified cross-sections quite well with a correlation coefficient above 0.99, in particular for molybdenum (Table 1).

Table 1. Approximation values and theoretical correlations for protons in Mo

E_0, [MeV]	σ_0	a	E_0	k	η
1	17176	0.22	4.39	5600	0.999
5	2919	0.0249	31.35	3719	0.9999
10	2123	1.45	1.06	42.1	0.999
15	1694	2.68	0.84	16.92	0.999
20	1413	2.33	1.23	15.19	0.997
25	1227	1.89	1.85	15.64	0.99
30	1067	1.60	2.43	15.01	0.996
40	912.2	0.13	37.98	142.36	0.996
50	790.3	0.11	53.77	136.92	0.99

Let us consider some properties of CPF taking into account the energy loss for protons and alpha particles.

1) $\lim\limits_{h'\to 0}\psi_n\left(h,E_0\right)=\dfrac{1}{n!\lambda_0^n}\left(\dfrac{E_0}{E_0-kh}\right)^{-l}\exp\left(-\dfrac{h}{\lambda_0}\right)\left(h+\dfrac{\ln\left(\dfrac{E_0}{E_0-kh}\right)}{ak}\right)^n$,

2) $\lim\limits_{k\to 0}\psi_0\left(h',h,E_0\right)=\exp\left(-\dfrac{h-h'}{\lambda}\right)$, $\lim\limits_{k\to 0}\psi_n\left(h',h,E_0\right)=\dfrac{\left(h-h'\right)^n}{n!\lambda^n}\exp\left(-\dfrac{h-h'}{\lambda}\right)$,

where $\dfrac{1}{\lambda}=\dfrac{1}{\lambda_0}\left(1+\dfrac{1}{aE_0}\right)$.

3) Extremes, areas of decrease and increase.

Find the derivative of $\psi_0^{'}\left(h',h,E_0\right)$ with respect to h:

$$\psi_0^{'}\left(h',h,E_0\right)=\left[\left(\frac{E_0-kh'}{E_0-kh}\right)^{-l}\exp\left(-\frac{h-h'}{\lambda_0}\right)\right]_h^{'}=\frac{1}{\lambda_0}\left(\frac{E_0-kh'}{E_0-kh}\right)\exp\left(-\frac{h-h'}{\lambda_0}\right)*$$

$$*\left[\frac{-1}{a\left(E_0-kh\right)}-1\right];$$

at $-\dfrac{1}{a\left(E_0-kh\right)}+1=0$ $\quad\psi_0^{'}\left(h',h,E_0\right)=0$,

therefore $h = E_0/k + 1/ak$ is the point of the extremum.

If $h < E_0/k + 1/ak$, the function $\psi_0(h', h, E_0)$ decreases monotonously, and at $h > E_0/k + 1/ak$ increases monotonously, in this case $h_e = E_0/k + 1/ak$ is the point of minimum.

At $h = E_0/k + 1/ak$

$$\psi_0\left(h_э,h',E_0\right)=\left[a\left(E_0-kh'\right)\right]^{-\frac{1}{\lambda_0 ak}}\exp\left(\frac{-aE_0-1+h'ak}{\lambda_0 ak}\right).$$

At $n \geq 1$ the equation $d\psi_n/dh = 0$ can be solved only numerically. The point of minimum $h_e = E_0/k + 1/ak$ does not belong to the definition area of $\psi_n(h', h, E_0)$, since $h_e > h_{max}$ and therefore was not taken into account.

4) Inflection points, the intervals of convexity and concavity. Let us find ψ_0'' and equate it to zero. The equation $d^2\psi_0/dh^2 = 0$ takes place when

$$\left(\frac{E_0}{E_0-kh}\right)^2+\frac{2}{\lambda_0 a}\left(E_0-kh\right)+\left[\frac{1}{\lambda_0 a^2}-\frac{k}{a}\right]=0.$$

Solving this equation, we find:

$$h_1=\frac{E_0}{k}+\frac{\dfrac{2}{\lambda_0 a}+2\sqrt{\dfrac{k}{\lambda_0 a}}}{\lambda_0\,k/a};\ h_2=\frac{E_0}{k}+\frac{\dfrac{2}{\lambda_0 a}+2\sqrt{\dfrac{k}{\lambda_0 a}}}{\lambda_0\,k/a}.$$

Since the derivative ψ_0'' does not change the sign near points h_1 and h_2 ($\psi_0'' > 0$), the found points are not inflection ones.

5) Asymptotes. To find the vertical asymptotes, we calculate:

$$\lim_{h\to E_0/k} \frac{1}{n!\lambda_0^n}\left(\frac{E_0-kh'}{E_0-kh}\right)^{-l} \exp\left(-\frac{h-h'}{\lambda_0}\right)\left(h-h'+\frac{\ln\left(\frac{E_0-kh'}{E_0-kh}\right)}{ak}\right)^n = 0.$$

$$\lim_{h\to E_0/k} \psi_n\left(h', h, E_0\right) = 0.$$

Consequently, $h = E_0/k$ is not a vertical asymptote for protons and alpha particles. Obviously, there are no inclined and horizontal asymptotes too, since $h' \le h \le h_{max}$. The remaining properties of CPF for protons and alpha particles are the same as the properties of the cascade-probability function, which takes into account the energy loss for electrons.

For large values of *n*, CPF calculations were performed using the following modified formula:

$$\psi_n\left(h', h, E_0\right) = \exp\left(-n\lambda_0 - \ln n! - \frac{1}{\lambda_0 ak}\ln\left(\frac{E_0-kh'}{E_0-kh}\right) - \frac{h-h'}{\lambda_0}\right) + n\ln\left(h-h'+\frac{1}{ak}\ln\left(\frac{E_0-kh'}{E_0-kh}\right)\right). \quad (5)$$

The software package for calculating CP-functions and selecting the type of theoretical curves is implemented in a Python environment using the Django framework. The calculations are made for protons and α-particles in various targets. As an example, Figures 2 and 3 show the dependence of CPF on the number of interactions and the penetration depth for alpha particles in Mo at E_0 = 10 MeV.

The calculations show that with values of n = 0,1 CPF decrease, depending on *h*, with increasing *n*, they increase, reaching a maximum and begin to decrease. As E_0 grows, the curves shift to the right.

Further to that, the energy spectra of PKA were calculated with formula (3), in particular, for α-particles in Mo. It can be seen that they are decreasing functions (Figs. 4,5). In a good approximation, W (E_2) ~ 1/E_2.

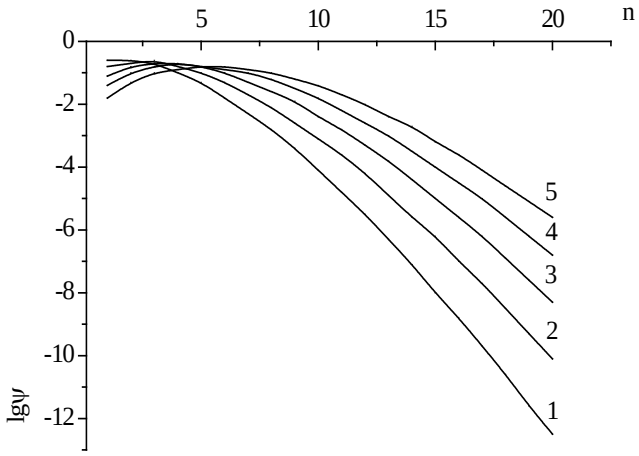

Fig. 2. Dependence of CPF on the number of interactions for alpha particles in molybdenum at E_0 = 10 MeV, *h* = 0.006; 0.008; 0.01; 0.012; 0.014 cm (1-5)

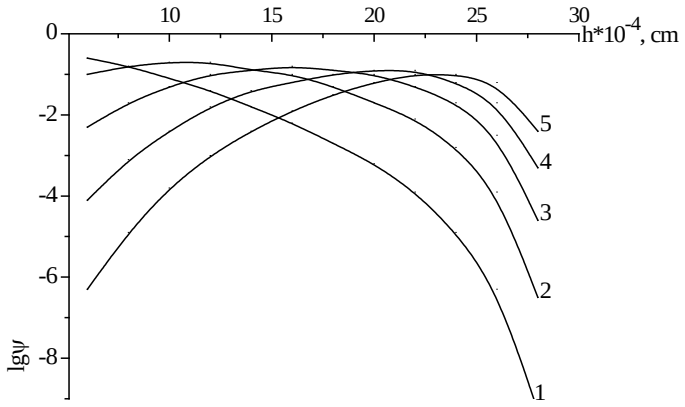

Fig. 3. Dependence of CPF on the penetration depth for alpha particles in molybdenum at E_0 = 10 MeV; n = 1, 4, 7, 10, 13 (1-5)

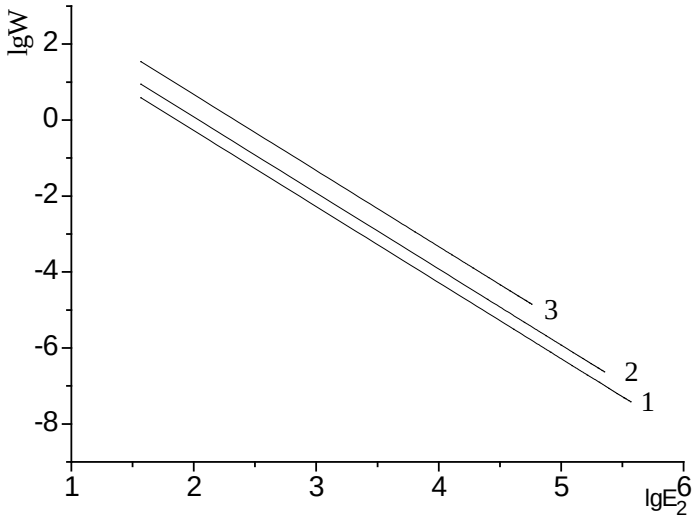

Fig. 4. Dependence $W(E_0, E_2, h)$ for protons in Mo at E_0 = 10 MeV on E_2 at the depths: h = 40 μm (1), h = 156 μm (2), h = 238 μm (3)

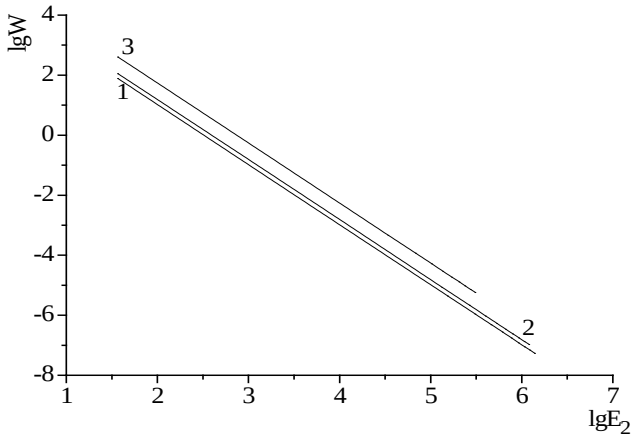

Fig. 5. Dependence $\omega(E_0, E_2, h)$ for α-particles in Mo at E_0 = 10 MeV on E_2 at the depths: h = 4 μm (1), h = 10 μm (2), h = 25 μm (3)

Using formula (4), the concentrations of vacancy clusters were calculated at E_0 = 10, 50 MeV. With increasing depth h, C_k increases, and at the end of the run, it drops sharply to zero. With increasing E_c, the concentration of clusters decreases (Figs. 6 and 7).

Earlier, we calculated the dependence of C_k on h under proton irradiation, which are in satisfactory agreement with experiments on two-photon positron annihilation [2].

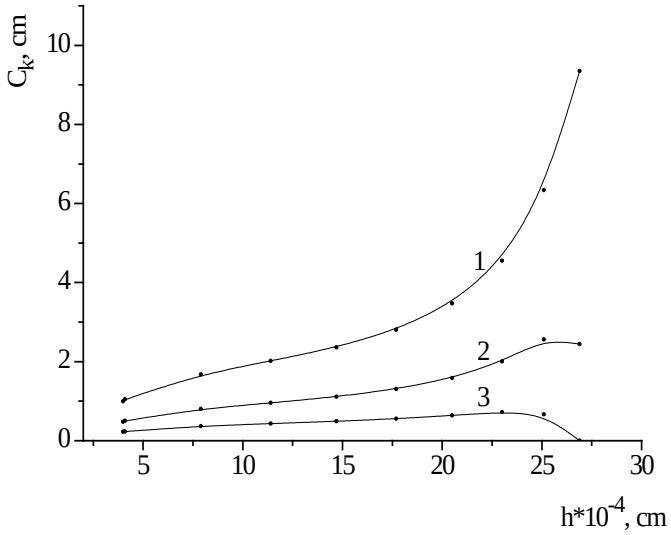

Fig. 6. Dependence of the vacancy clusters concentration on the penetration depth for alpha particles in molybdenum at E_0 = 10 MeV, E_C = 50, 100, 200 keV (1-3)

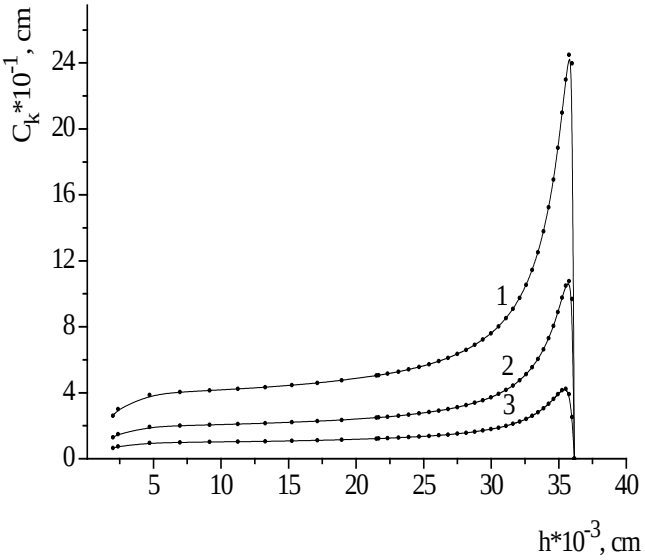

Fig. 7. Dependence of the vacancy clusters concentration on the penetration depth for alpha particles in molybdenum at E_0 = 50 MeV, E_C = 50, 100, 200 keV (1-3)

4. Conclusions

- The analysis of modified cross-sections and the calculation of cascade-probability functions for protons and alpha particles were carried out. It was shown that the correlation coefficients $\eta > 0.99$ (calculated and modified values), which is a good approximation.
- CPF was analyzed and its main properties were established. When k = 0, this function goes to the simplest CPF. There are inflection points and maxima. With increasing n, CPF increases, reaches a maximum, and further decreases. As h increases, the maxima of the curves shift to the right.

- The energy spectra of PKA in Mo were calculated. In a good approximation, we have $W(E_2) \sim 1/E_2$. With increasing depth, C_k increases slowly, reaches a maximum near the end of the path and drops sharply to zero. With increasing E_c, C_k decreases.

References

1. Agranovich VM, Kirsanov VV. Simulation problems of radiation defects in crystals. *Uspekhi Fizicheskikh Nauk*. 1976;118(1): 3-51.
2. Melker AI. *Dynamics of Condensed Matter, Vol. 2, Collisions and Branchings.* St. Petersburg Academy of Sciences on Strength Problems; 2010.
3. Aleksandrov OV, Visotskaya SA, Zhurkin VS. Model of charge of accumulation in MOS-transistors at ionizing irradiation. *Izvestiya St. Petersburg State Electrotechnical University «LETI»*. 2012;7: 20-27.
4. Bogatyrev YuV, Lastovsky SB, Soroka SA, Shwedov SV, Ogorodnikov DA. Influence of gamma radiation on MOS/SOI transistors. *Reports of BGUIR*. 2016;3(97): 75-80.
5. Melker AI. Creation and evolution of vacancy clusters in solids under irradiation. Theory and computer simulation. In: *AIP Conference Proceedings 303: Slow Positron Beams Technique for Solids and Surfaces.* Ottewitte E, Weiss AH. (Eds.) New York: American Institute of Physics; 1994. p.156-178.
6. Kharlamov VS, Kulikov DV, Lubov MN, Trushin YuV. Kinetic Modeling of the growth of copper clusters of various heights in subsurface layers of lead. *Tech. Phys. Lett.* 2015;41: 961-963.
7. Komarov FF, Milchanin OV, Skuratov VA, Mokhovikov MA, Janse A.van Vuuren, Neethling JN, Wendler E, Vlasukova LA, Parkhomenko IN, Yuvchenko VN. Ion-beam formation and track modification of InAs nanoclusters in silicon and silicon dioxide. *Proceedings of the Russian Academy of Sciences. Physical series*. 2016;80(2): 165-169.
8. Ivchenko VA. Atomic structure of cascades of atomic displacements in metals and alloys after different types of radiation. *IOP Conf. Series: Materials Science and Engineering.* 2016;110: 012003.
9. Velichko OI. Modeling of the transient interstitial diffusion of implanted atoms during low temperature annealing of silicon substrates. *Physica B.* 2012;407: 2176-2184.
10. Pogrebnjak AD, Yakushenko IV, Bondar OV, Sobol OV, Beresnev VM, Oyoshi K, Amekura H, Takeda Y. Influence of implantation of Au– ions on the microstructure and mechanical properties of the nanostructured multielement (TiZrHfVNbTa)N coating. *Phys. Solid State.* 2015;57(8): 1559-1564.
11. Kozlova OA, Zelenina MS. Ab initio simulation of two-dimensional MOS_2 with vacancy clusters using grid technologies. *Materials Physics and Mechanics.* 2014;20(1): 51-55.
12. Boos EG, Kupchishin AI, Kupchishin AA, Shmygalev YeV, Shmygaleva TA. *Cascade-probabilistic method. Solution of radiation-physical problems, Boltzmann equations. Connection with Markov's chains*. Almaty, Abay KazNPU, SRINCTaM al-Farabi KazNU, Kama LLP, 2015.
13. Kupchishin AI, Shmygalev EV, Shmygaleva TA, Jorabayev AB. Relationship between Markov Chains and Radiation Defect Formation Processes by Ion Irradiation. *Modern Applied Science*. 2015;9(3): 59-70.
14. Nelaev VV, Stempitsii VR. *Osnovy SAPR v mikroelektronike. Fizicheskoe modelirovanie tekhnologii i pribora: uchebnoe posobie*. Minsk: BSUIR; 2006.
15. Kupchishin AI, Voronova NA, Shmygaleva TA, Kupchishin AA. Computer simulation of vacancy clusters distribution by depth in molybdenum irradiated by alpha particles. *Key Engineering Materials.* 2018: 3-7.
16. Sogojan AV. Space Model. *M: MS University, Institute of Nuclear Physics*. 2007;2: 3-7.

17. Makhavikou M, Komarov F, Parkhomenko I, Vlasukova L, Milchanin O, Zuk J, Wendler E, Romanov I, Korolik O, Togambayeva A. Structure and optical properties of SiO_2 films with ZnSe nanocrystals formed by ion implantation. *Surface Coatings Technology*. 2018: 596-600.
18. Makhavikou M, Parkhomenko I, Vlasukova L, Komarov F, Milchanin O, Mudryi A, Zhivulko V, Wendler E, Togambayeva A, Korolik O. Raman monitoring of ZnSe and ZnS_xSe_{1-x} nanocrystals formed in SiO_2 by ion implantation. *Nuclear, Instruments and Methods in Physics Research Section B: Beam Interactions with Materials and Atoms.* 2018: 1-4.
19. Klimovicha IM, Komarov FF, Zaikova VA, Kuleshova AK, and Pilkob VV. Influence of Parameters of Reactive Magnetron Sputtering on Tribomechanical Properties of Protective Nanostructured Ti–Al–N Coatings. *Journal of Friction and Wear*. 2018;39(2): 92-98.
20. Boucard FA. Comprehensive solution for simulating ultra−shallow junctions: From high dose/low energy implant to diffusion annealing. *Mater. Sci. and Eng. B.* 2005;124-125: 409-414.

THE AUTHORS

Natalia A. Voronova
e-mail: nataliya.voronova@irb.rest
ORCID: -

Alexander A. Kupchishin
e-mail: -
ORCID: -

Anatoly I.Kupchishin
e-mail: ankupchishin@mail.ru
ORCID: 0000-0002-8872-3734

Tatiana A. Shmygaleva
e-mail: shmyg1953@mail.ru
ORCID: 0000-0001-6750-253X